Template Catalysis by Metal−Ligand Cooperation. C−C Bond Formation via Conjugate Addition of Non-activated Nitriles under Mild, Base-free Conditions Catalyzed by a Manganese Pincer Complex

Alexander Nerush,[†,§] Matthias Vogt,[†,#,§] Urs Gellrich,[†,§] Gregory Leitus,[‡] Yehoshoa Ben-David,[†] and David Milstein*,[†]

[†]Department of Organic Chemistry and [‡]Department of Chemical Research Support, The Weizmann Institute of Science, Rehovot 76100, Israel

[#]Institut für Anorganische Chemie und Kristallographie, Universität Bremen, Leobener Straße, 28359 Bremen, Germany

S *Supporting Information*

ABSTRACT: The first example of a catalytic Michael addition reaction of non-activated aliphatic nitriles to α,β-unsaturated carbonyl compounds under mild, neutral conditions is reported. A new de-aromatized pyridine-based PNP pincer complex of the Earth-abundant, first-row transition metal manganese serves as the catalyst. The reaction tolerates a variety of nitriles and Michael acceptors with different steric features and acceptor strengths. Mechanistic investigations including temperature-dependent NMR spectroscopy and DFT calculations reveal that the cooperative activation of alkyl nitriles, which leads to the generation of metalated nitrile nucleophile species (α-cyano carbanion analogues), is a key step of the mechanism. The metal center is not directly involved in the catalytic bond formation but rather serves, cooperatively with the ligand, as a template for the substrate activation. This approach of "template catalysis" expands the scope of potential donors for conjugate addition reactions.
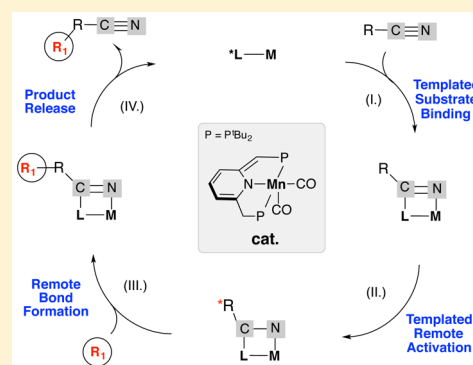
INTRODUCTION

Conjugate addition reactions are fundamental C−C bond formation reactions in organic chemistry.[1] For instance, the Michael addition of 1,3-dicarbonyl compounds to activated olefins is regarded as one of the most important C−C coupling reaction in organic synthesis.[2] However, such Michael reactions require the application of strong bases, which may not be compatible with various functional groups and can lead to undesired side reactions. Transition-metal-catalyzed Michael-type reactions have been reported that can operate under mild and neutral conditions and exhibit superior chemoselectivity.[2,3]

Nitriles are important functional groups in organic synthesis due to their facile transformation into various functional groups. Furthermore, nitriles themselves are important constituents of modern pharmaceuticals. In 2010, more than 30 nitrile-containing drugs were on the market, and more than 20 leads containing nitrile functionalities were in clinical development.[4] Common protocols for conjugate addition reactions involving nitriles make use of activated nitriles with acidic α-protons (e.g., malononitriles, benzyl cyanide, ethyl cyanoacetates, cyanoacetamides, and the like). The same applies for previously reported transition-metal-catalyzed Michael addition reactions, therefore significantly limiting the substrate scope. The reaction usually involves C−H activation

at the α-carbon at the metal center to generate the Michael donor moieties (i.e., metal stabilized carbanions).[5−10] Fleming and co-workers discussed the stereochemical aspects of α-lithiation and α-magnesation of nitriles with strong bases.[6,11] In an early report Rappoport and co-workers described the utilization of a large excess of tetraethylammonium fluoride to generate cyanmethide carbanions from acetonitrile and use them in Michael addition reactions.[12] An example making use of the bifunctional reactivity of Ru- and Ir-based amido complexes to activate α-substituted α-cyano acetates was reported by Ikariya and co-workers.[13]

Non-activated aliphatic nitriles have also been used in transition-metal-catalyzed C−C bond-forming reactions. However, due to the low acidity of the α-protons of aliphatic nitriles, no conjugate addition of nitriles to α,β-unsaturated carbonyl compounds has been achieved so far. The accomplishments in C−C bond-forming reactions of alkyl nitriles are summarized in a very recent review.[14]

Recently, we reported a complementary approach for transition-metal-catalyzed addition of nitriles to α,β-unsaturated carbonyl compounds. A de-aromatized PNP rhenium pincer

Scheme 1. Previously Reported Rhenium Pincer Complex-Catalyzed Addition of Benzylic Nitriles to Michael Acceptors, and Conjugate Addition of Non-activated Aliphatic and Benzylic Nitriles Catalyzed by Pincer Complex 4 of Earth-Abundant Manganese
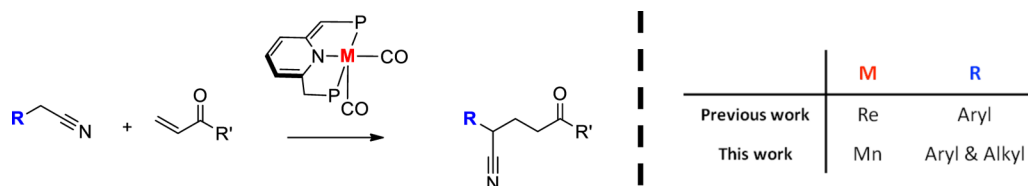
complex was used as catalyst (Scheme 1). Stoichiometric reactions of this de-aromatized rhenium-pincer complex with benzylic nitriles showed that an initial [1,3]-addition of the nitrile with C−C and Re−N bond formation occurs. A subsequent tautomerization of the formed ketimido complex leads to an enamido complex. This enamido complex is assumed to be the actual nucleophile for the Michael addition. With regard to the substrates, the rhenium pincer complex catalyzed conjugate addition was limited to benzylic nitriles.[15] Later, Pidko and co-workers described a pyridine-based Ru-CNC carbene pincer complex, which, upon application of phosphazene base, cooperatively binds acetonitrile and benzonitrile via a similar [1,3]-addition reaction under C−C and N−Ru bond formation.[16] Otten, de Vries, and co-workers reported an oxa-Michael addition reaction of alcohols to unsaturated nitriles[17] utilizing a pyridine-based de-aromatized ruthenium PNN pincer complex.

There is a strong current interest in replacing noble metal catalysts by abundant and inexpensive base-metal catalysts. Manganese is one of the most abundant transition metals on Earth's crust, third only to iron and titanium. We report here the synthesis of a PNP pincer-type manganese complex, ([Mn(PNP^{tBu})(CO)$_3$]Br (2, PNP^{tBu} = 2,6-bis(di-*tert*-butylphosphinomethyl)pyridine). This complex undergoes facile deprotonation at the *exo*-cyclic methylene carbon moiety to yield a de-aromatized complex [Mn(PNP^{tBu}*)(CO)$_2$] (4) (the asterisks denotes de-aromatized PNP ligand), capable of the catalytic activation of nitriles, including non-activated aliphatic nitriles, toward Michael acceptors under neutral conditions (Scheme 1). Notably, this transformation is difficult even under basic conditions.[18]

To the best of our knowledge this is the first example of a first-row transition-metal-catalyzed Michael addition of non-activated aliphatic nitriles.

This nitrile activation is triggered by metal−ligand cooperation (MLC), in which the manganese center, as well as the coordinated PNP-pincer ligand, participate synergistically in a stepwise chemical bond activation process. MLC has been developed into a versatile tool for chemical bond activation.[19−25] Transition metal complexes with pyridine- and acridine-based LNL′-type (L = N or P) pincer ligands exhibit MLC based on aromatization/de-aromatization[26] of the pincer ligand, resulting in facile activation of various X−H single bonds, including N−H,[27,28] O−H,[29] H−H,[30−32] C−H,[32−36] and S−H[37,38] bonds. In contrast to the X−H (X = C, H, N, O, S) heterolytic single bond activation via MLC, multiple bonds can be activated but not entirely cleaved. Instead, a reduction in bond order is observed. For instance, the activation of C═O bonds results in a C−O single bond, with concomitant formation of a C−C bond between the carbonyl carbon and the *exo*-cyclic methine carbon of the pincer "arm" as well as formation of a M−O bond. We[39−41] and others[42−44] have

previously reported on the activation of C═O double bonds, including also a novel binding mode of CO$_2$ to a metal complex.

In general, well-defined pincer complexes of Mn are scarce in the literature. Reports comprise Mn(I) PNP compounds published by Nocera and Ozerov,[45] a Mn(II) center with pyridine-based NNN-pincer motif bearing two pyrazole "arms",[46] and Mn-PDI (PDI = 2,6-bisimino pyridine) species described by Chirik and co-workers.[47]

■ RESULTS AND DISCUSSION

Complex 2 is readily obtained upon stirring a solution of 2,6-bis(di-*tert*-butylphosphinomethyl)pyridine (PNP^{tBu}, 1) and [Mn(CO)$_5$Br] for 30 h at ambient temperature (Scheme 2).

Scheme 2. Synthesis of Mn PNP Pincer Complexes 2−4 (P = ^{t}Bu$_2$P)
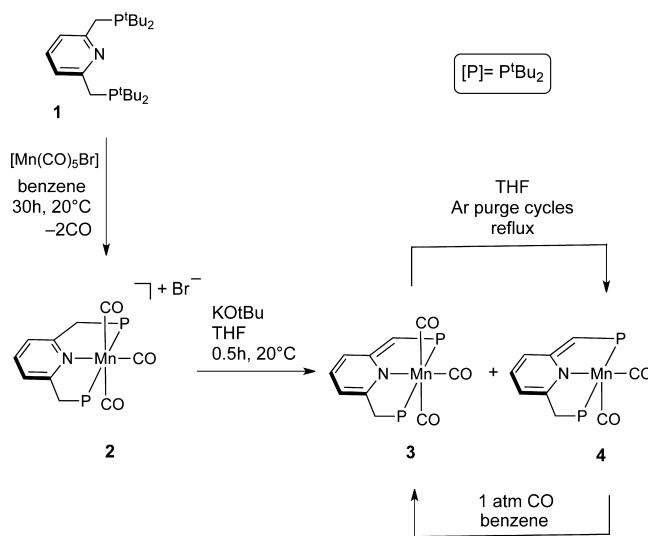
Subsequent precipitation from benzene by addition of *n*-pentane gives complex 2 as a yellow powder in 83% yield. In contrast to our previously reported isoelectronic rhenium complex *cis*-[Re(PNP^{tBu})(CO)$_2$Cl], complex 2 forms a cationic tris-carbonyl complex with a bromide counteranion. The IR spectrum exhibits absorption bands characteristic of an octahedral tris-carbonyl complex in a meridional arrangement (absorption maxima at 1919, 1932 cm^{-1} (partly overlapping) for $\nu_{asym} + \nu_{asym'}$ and at 2021 cm^{-1} for ν_{sym}). The ^{31}P{^{1}H} NMR spectrum of 2 exhibits a singlet at 109.4 ppm, indicating two chemically equivalent phosphorus nuclei. The ^{13}C{^{1}H} NMR spectrum shows two triplet resonances at 220.5 ppm (t, $^2J_{CP}$ = 15.9 Hz) for two chemically equivalent carbon nuclei in mutual *trans*-positions (apical) and at 223.9 ppm (t, $^2J_{CP}$ = 12.8 Hz) for one carbon nucleus in the *trans*-position with respect to the

pyridine unit. Upon addition of 1 equiv of the base KO^{t}Bu to a suspension of **2** in THF, a color change from yellow to brown is observed, and a solution comprising a mixture of the de-aromatized tris- and bis-carbonyl compounds *mer*-[Mn-(PNP^{tBu}*)(CO)$_3$] (**3**) and *cis*-[Mn(PNP^{tBu}*)(CO)$_2$] (**4**) is obtained in 2:1 ratio. However, complex **4** can be obtained as the sole product upon heating the reaction mixture of **2** and KO^{t}Bu in THF under vigorous reflux. Extraction with *n*-pentane and subsequent recrystallization at −38 °C gives the complex *cis*-[Mn(PNP^{tBu}*)(CO)$_2$] (**4**) as a deep blue solid in 60% yield. The IR spectrum of **4** (KBr pellet) shows two strong absorptions at 1833 (ν_{asym}) and 1904 cm^{-1} (ν_{sym}), signifying the formation of a dicarbonyl species. The ^{31}P{^{1}H} NMR spectrum indicates a reduced symmetry with respect to complex **2**. The spectrum exhibits an AB-spin system, suggesting that the two phosphorus nuclei are chemically inequivalent with doublets at 87.2 and 101.3 ppm and a $^2J_{PP}$ coupling constant of 68 Hz. Consistently, the ^{1}H NMR spectrum exhibits three distinct resonances in the aromatic regime, signifying the reduction in symmetry, particularly the loss of the mirror plane perpendicular to the pyridine ring. The three resonances are shifted to lower frequencies (5.45, 6.36, and 6.40 ppm). As a result of the deprotonation of one *exo*-cyclic methylene group, the ^{1}H NMR spectrum shows two resonances for the pincer "arm" protons: a doublet at 2.77 ppm ($^2J_{HP}$ = 9.2 Hz) for the two equivalent *CH$_2$* protons and a broad singlet at 3.82 ppm for the methine *CH* proton. Two sharp doublet resonances (1.00 and 1.28 ppm) are observed for the methyl groups of the four P(^{t}Bu)$_2$ moieties, with $^2J_{HP}$ = 12.7 and 13.0 Hz, respectively. Consistently, only one resonance is observed in the carbonyl regime in the ^{13}C{^{1}H} NMR spectrum for both CO ligands (239.3 ppm, $^2J_{CP}$ = 17 Hz), indicating two chemically equivalent carbon nuclei. These findings suggest the existence of a mirror plane through the PNP pyridine ring and corroborate a trigonal bipyramidal coordination sphere around the manganese center or a fast dynamic interconversion of two equivalent square pyramidal structures with respect to the NMR time scale. Single crystals suitable for an X-ray diffraction study were obtained from a concentrated solution of **4** in *n*-pentane. The molecular structure of **4** is shown in Figure 1. The tridentate pincer ligand PNP^{tBu} binds the Mn(I) center in a meridional fashion. The two carbonyl ligands are located in mutual *cis*-positions (C−Mn−C = 86.5°), completing a distorted square pyramidal coordination sphere around the Mn center. Carbon monoxide binds reversibly to complex **4**. Thus, the tris-carbonyl starting material *mer*-[Mn(PNP^{tBu}*)(CO)$_3$] (**3**) is readily obtained, when a solution of **4** in C$_6$D$_6$ is subjected to 1 atm of CO gas; the unsaturated **4** is regenerated upon refluxing in THF (Scheme 2).

Reaction of Complex 4 with Nitriles Bearing α-CH$_2$ Groups. The penta-coordinated de-aromatized complex **4** reacts with benzyl cyanide with formation of C−C and Mn−N bonds owing to a [1,3]-addition reaction mediated by a de-aromatization/aromatization pathway (Scheme 3). Upon addition of 2 equiv of benzyl cyanide to a deep blue solution of **4** in THF, a drastic color change to red is observed. Recrystallization from THF/*n*-pentane at −38 °C gives the enamido complex *cis*-[Mn(PNP^{tBu}-HNCH═CHPh)(CO)$_2$] (**5**) as large red crystals in 85% yield. The ^{31}P{^{1}H} NMR spectrum of **5** shows the expected two doublets of the AB-spin system for two phosphorus nuclei in different chemical environment at higher frequencies (126.6 and 140.1 ppm)
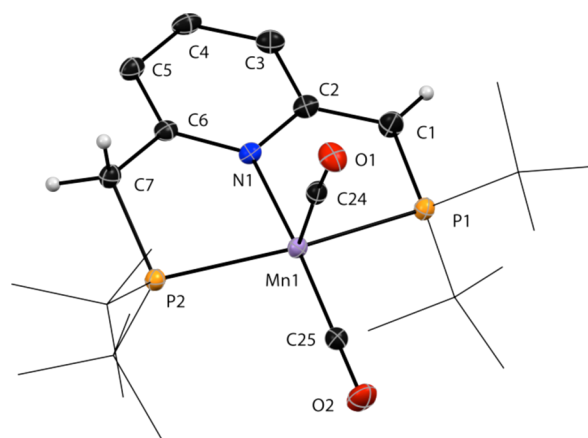

Figure 1. ORTEP diagram of *cis*-[Mn(PNP^{tBu}*(CO)$_2$] (**4**) with thermal ellipsoids at 30% probability. The P(^{t}Bu)$_2$ groups are drawn as wire frames, and hydrogen atoms are partially omitted for clarity. Selected bond lengths: C1−C2 = 1.369(3) Å, C2−C3 = 1.449(3) Å, C3−C4 = 1.348(3) Å, C4−C5 = 1.407(3) Å, C5−C6 = 1.373(3) Å, C6−C7 = 1.498(3) Å, Mn1−N1 = 2.0333(16) Å, Mn1−P1 = 2.2950(7) Å, Mn1−P2 = 2.3117(7) Å, Mn1−C24 = 1.744(2) Å, Mn1−C25 = 1.768(2) Å, C24−O1 = 1.168(2) Å, C25−O2 = 1.171(2) Å.

and with a significantly larger coupling constant with respect to the de-aromatized complex **4** ($^2J_{PP}$ = 100 Hz in **5** vs 68 Hz in **4**). The ^{1}H NMR resonances centered at 4.39 ppm (s, amido 1H, Mn−N*H*) and 5.41 (s, olefinic 1H, C═C*H*Ph) indicate the formation of an enamido motif in **5**. The carbonyl stretches in the IR spectrum (KBr pellet) appear at 1832 and 1905 cm^{-1} in a 1:1 ratio, signifying a mutual *cis*-arrangement of both carbonyls.

An X-ray diffraction study of crystals of the enamido complex **5** (Figure 2) exhibits a distorted octahedral coordination sphere, formed by the meridional PNP^{tBu} pincer ligand and two CO ligands in mutual *cis*-positions and the amido moiety in an axial position. A short C26−C27 interatomic distance (1.383 Å) typical of a C═C double bond is observed, accompanied by a long C26−N2 (1.345 Å) bond indicating a C−N single bond adjacent to an sp^2-hybridized carbon. The [1,3]-addition of benzyl cyanide to **4** to form **5** is characterized by the newly formed C−C single bond between the *exo*-cyclic carbon of the pincer (C7−C26 = 1.540 Å) and a Mn−N bond (Mn1−N2 = 2.058 Å).

The [1,3]-addition of benzyl cyanide to **4** with C−C and Mn−N bond formation is reversible. This is clearly demonstrated when a solution of complex **5** in benzene is treated with 1 atm of CO gas at ambient temperature. The de-aromatized tris-carbonyl complex **3** is readily formed with concomitant displacement of benzyl cyanide. The reaction can be conveniently followed by ^{31}P{^{1}H} NMR spectroscopy. Representative spectra of the transformation of **5** into **3** are shown in Figure 3.

Catalytic Michael Reactions. As shown above, *cis*-[Mn(PNP^{tBu}*)(CO)$_2$] (**4**) readily reacts with benzyl cyanide to form the enamido complex **5**. Both compounds **4** and **5** are potent catalysts for the Michael addition of benzyl cyanide to ethyl acrylate. At ambient temperature in benzene, ethyl 4-cyano-4-phenylbutanoate is obtained within 12 h in 90% and 93% yield, respectively (1 mmol scale, 1:1 substrate ratio, Scheme 4).
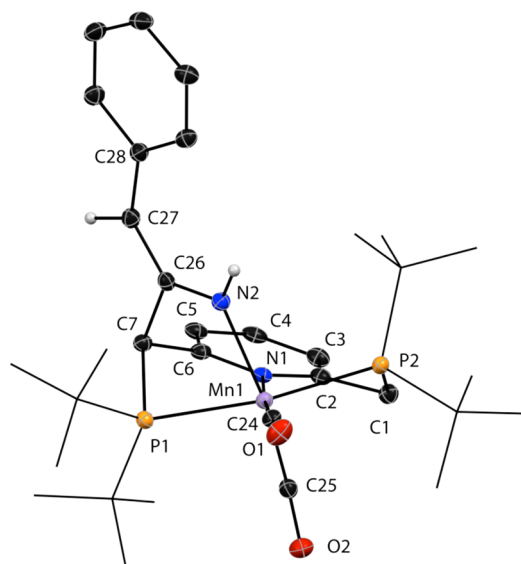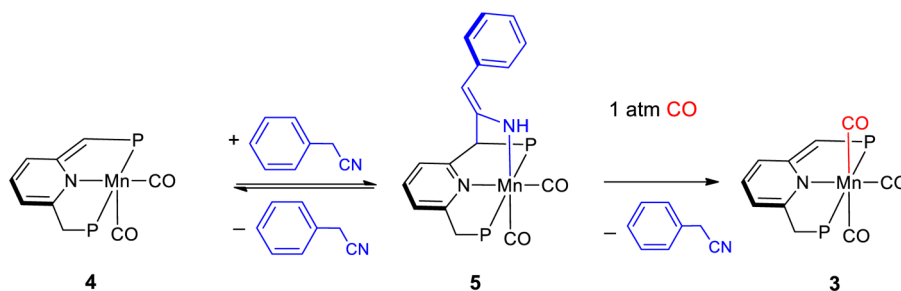
Scheme 3. Reversible Binding of Benzyl Cyanide to Complex 4 (P = ᵗBu₂P)

Figure 2. ORTEP diagram of *cis*-[Mn(PNP^tBu-HNCH=CHPh)-(CO)₂]·THF (**5**) with thermal ellipsoids at 30% probability. The co-crystallized THF solvent molecule is omitted. The P(*tert*-butyl)₂ groups are drawn as wire frames, and hydrogen atoms are partially omitted for clarity. Selected bond lengths: C1−C2 = 1.502(3) Å, C2−C3 = 1.385(3) Å, C3−C4 = 1.387(3) Å, C4−C5 = 1.375(3) Å, C5−C6 = 1.390(3) Å, C6−C7 = 1.499(3) Å, C7−C26 = 1.540(3) Å, C26−C27 = 1.383(3)Å, C27−C28 = 1.446(3) Å, C26−N2 = 1.345(2) Å, Mn1−N1 = 2.0519(16) Å, Mn1−N2 = 2.058(2) Å, Mn1−P1 = 2.3241(7) Å, Mn1−P2 = 2.3254(8) Å, Mn1−C24 = 1.766(2) Å, Mn1−C25 = 1.780(2) Å, C24−O1 = 1.173(3) Å, C25−O2 = 1.167(2) Å.

Screening of different solvents showed that nonpolar solvents such as *n*-pentane and benzene are most suitable for the catalytic reaction (for details of solvent screening, see Supporting Information, p S10).

Importantly, a variety of aliphatic nitriles (R−CN with R = Me, Et, *n*-Pr, *n*-Bu, Table 1, entries 1−5) undergo facile Michael addition to ethyl acrylate catalyzed by complex **4** (0.5 mol%). The catalytic reactions were performed on a 2.5 mmol scale with a nitrile:ethyl acrylate ratio of 1:1, using benzene as solvent. The *γ*-cyanoesters were obtained in moderate to excellent yields. A common observed side product was the double addition product of two nitrile donors to ethyl acrylate, resulting in moderate yields for the addition reactions of acetonitrile (entry 1) to ethyl acrylate. When acetonitrile was also used as solvent (entry 2), the mono-addition product was formed exclusively. Remarkably, the addition reaction of propionitrile to ethyl acrylate occurs very selectively in high yield and short reaction time (entry 3).

We have also explored the scope of *α,β*-unsaturated carbonyl compounds as suitable acceptors. Table 2 exhibits our results for reactions of propionitrile with various acrylates, methyl crotonate, and cyclohex-2-enone (entries 1−8). The reactions were performed on a 1 mmol scale with respect to the Michael acceptor. The reactions given in entries 4−8 were performed in neat propionitrile as solvent. The reaction tolerates ketones (entry 2) as well as flourinated esters (entry 3); however, the reaction with phenyl acrylate proceeds at a slow rate (entry 4). The effect of terminal substitution of the double bond in the Michael acceptor is significant. Reduction in the reaction rate and selectivity was observed upon addition of propionitrile to *trans*-methyl crotonate (entry 8). After an extended reaction time of 24 h, only 40% conversion of the crotonate was detected, and the desired addition product was formed in only 18% yield. In contrast, acceptors bearing a substituted terminal double bond react well. Thus, under the same reaction conditions, methyl methacrylate (entry 5) showed full conversion already after 12 h, with the product obtained in 92% yield. Similarly, trifluoroethyl methacrylate resulted in 93% yield after 5 h (entry 6). The very reactive Michael acceptor cyclohex-2-enone (entry 7) showed a tendency for homo-addition reactions to form [1,1′-bi(cyclohexan)]-6-ene-2,3′-dione, causing low yield of the desired product (for further details, see the Supporting Information, p S44).

Reaction of Aliphatic Nitriles with Complex 4. Most significantly, non-activated, aliphatic nitriles are suitable substrates for Michael-type C−C couplings catalyzed by complex **4**. We therefore investigated the binding of propionitrile to **4** by means of temperature-dependent NMR spectroscopy. The ³¹P{¹H} NMR spectrum of a solution containing complex **4** and 12 equiv of propionitrile in *n*-pentane at ambient temperature shows dynamic behavior, with broad resonances assigned to the de-aromatized complex **4** (d at 83.9 ppm and d at 98.9 ppm, $^2J_{PP}$ = 68 Hz). Upon cooling the sample stepwise to 235 K, a new set of doublets at 126.5 and 163.8 ppm appears (AB system with $^2J_{PP}$ = 107 Hz, Figure 4), indicating reversible binding of propionitrile to complex **4**. The following thermochemical parameters for the binding of propionitrile to complex **4** were derived from a van't Hoff plot: ΔH = −13.6 ± 1.2 kcal/mol and ΔS = −69 ± 5.0 cal/mol·K.

In contrast to the reaction of **4** with benzyl cyanide, the ³¹P{¹H} NMR spectrum of the reaction with propionitrile in *n*-pentane shows resonances significantly shifted to higher frequencies, when compared to the spectrum of **5** (d at 140.1 and 126.6 ppm), signifying the formation of a ketimido complex rather than an enamido species. Note that the ³¹P{¹H} NMR spectrum of the ketimido complex [Mn(PNP-N=CPh)(CO)₂], prepared from the reaction of **4** and benzonitrile has similar chemical shifts of the two phosphorus resonances
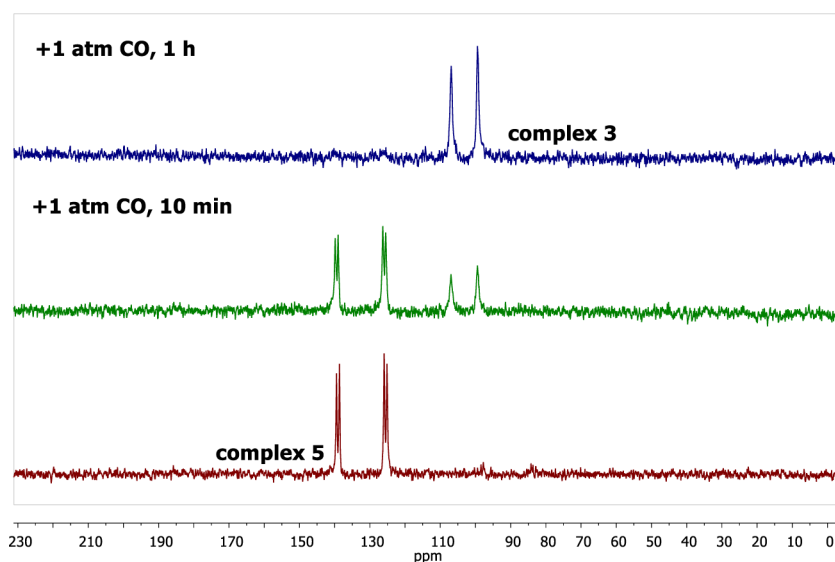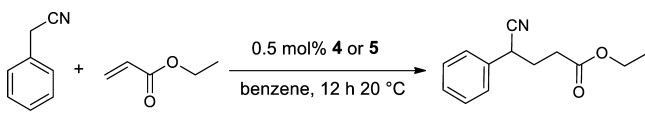
Figure 3. $^{31}P\{^1H\}$ NMR spectra of the reaction of complex **5** with 1 atm of CO in C_6D_6 at ambient temperature. Red, compound **5**; green, after addition of CO, 10 min; blue, after addition of CO, 1 h.

Scheme 4. Example of Michael Addition Catalyzed by Complex 4 or 5

(i.e., d at 165.6 and 126.5 ppm with $^2J_{PP}$ = 106 Hz); for NMR spectral details, see Supporting Information, p S9.

The $^{31}P\{^1H\}$ NMR spectrum of a sample of complex **4** dissolved in neat propionitrile shows similar broad resonances at room temperature. Cooling the sample stepwise to 225 K gives rise to the appearance of sharp resonances, consistent with the formation of the ketimido species **6** as the major compound (d, 128.1 and 166.0 ppm, $^2J_{PP}$ = 106 Hz). However, these resonances are accompanied by the formation of new signals, assigned to the enamido compound **7** as a minor species (d at 127.7 and 134.1 ppm, $^2J_{PP}$ = 106 Hz). Representative $^{31}P\{^1H\}$ NMR spectra are shown in Figure 5.

Evidently, propionitrile does not readily give the enamido compound **7**, unlike the reaction of **4** with benzyl cyanide, which results in the enamido complex **5**. However, there is evidence for the formation of an enamido moiety upon the reaction of **4** with a large excess of the nitrile at low temperature (Scheme 5). Temperature-dependent $^{31}P\{^1H\}$ NMR spin saturation transfer (SST) experiments in neat propionitrile show that the new species assigned to **7** is indeed in equilibrium with **6**, but the transfer from **6** to complex **4** remains predominant (for details, see Supporting Information). Undoubtedly, the enamido tautomer **5** is stabilized by conjugation with the aromatic ring, which is lacking in case of **7**. The finding that the spin saturation at low temperatures is exclusively transferred between **6** and **4** allowed us to determine the activation parameters for the transformation of **4** to **6** from $^{31}P\{^1H\}$ NMR SST experiments of a solution of **4** in toluene-d_8 in the presence of 12 equiv of propionitrile. The Eyring plot gives activation parameters of $\Delta H^‡$ = 11.7 ± 0.3 kcal/mol, $\Delta S^‡$ = −7.0 ± 1.4 cal/mol, and $\Delta G^‡$ = 13.8 ± 0.7 kcal/mol. Note that, in contrast to a solution in *n*-pentane, complex **7** can also be observed in a toluene-d_8 solution of **4** in

the presence of 12 equiv of propionitrile. However, as aforementioned, at low temperatures (222−247 K) mutual SST occurs exclusively between **4** and **6** (for details, see Supporting Information).

Computational Investigations. To allow for a better understanding of the elementary steps involved in the catalytic transformation, we performed DFT calculations at the TPSS-D3BJ/def2-TZVP//BP86-D3/def2-SV(P) level of theory. Since zwitterionic intermediates might be involved, both the geometry optimizations and the single-point energy calculations were performed using the SMD solvation model for benzene. Propionitrile and ethyl acrylate were chosen as representative substrates. The calculated binding of the substrate to **4** follows a mechanism similar to the one suggested for the analogous rhenium complex;[15] the nitrile first coordinates to **4** to give **8**, which can undergo C−C bond formation to give the aforementioned ketimido complex **6** (Figure 6).

The formation of **6** is predicted to be endergonic at 298 K but is computed to be slightly exergonic at 235 K (Scheme 6).

The calculated free energies agree with the observation made by NMR (Figure 4) that in the presence of an excess of propionitrile only **4** can be observed at 298 K, whereas **6** is detectable at 235 K. Furthermore, the computed ΔH value of −10.3 kcal/mol is in favorable agreement with the value derived from the van't Hoff analysis of the temperature-dependent NMR investigation in *n*-pentane (ΔH = −13.6 ± 1.2 kcal/mol). Also the activation barrier derived from DFT calculations ($\Delta G^‡$ = 11.7 kcal/mol) is in good agreement with the experimental data. Next, we investigated the tautomerism pathway leading to the enamide **7** (Figure 7). The ketimide nitrogen in complex **6** can be assumed to be basic; therefore, we commenced to elucidate whether it could deprotonate an acidic CH of a second propionitrile molecule. Starting from the hydrogen-bound complex **9**, a relaxed potential energy surface scan over the N···H distance did not yield a barrier. The zwitterionic complex **10** could be localized as a local minimum. A second proton transfer via **TS2** yields the tautomerized enamido complex **11**, to which the second propionitrile is bound via a N−H···N hydrogen bond.

Table 1. Michael Addition of Aliphatic Nitriles to Ethyl Acrylate Catalyzed by 4[a]

Entry	Nitrile	Time (h)	Conversion (%)	Yield (%)	Product
1	CN	20	69	26(21)	(product)
				20(17)	(product)
2	CN	40	90	89(83)	(product)
3	CN	6	>99	93(82)	(product)
4	CN	40	57	48(29)	(product)
5	CN	40	72	67(48)	(product)
6	CN	12	>99	94(84)	(product)
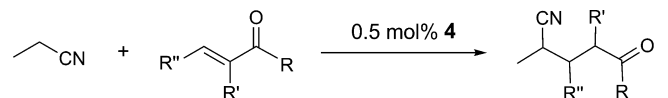
[a]Reaction conditions: A solution containing 2.5 mmol of the substrates in a 1:1 ratio and 0.5 mol% complex **4** in 2 mL of benzene was stirred under nitrogen at ambient temperature. For entry 2, acetonitrile was used as solvent. Conversion with respect to the ethyl acrylate was determined by ^{1}H NMR spectroscopic analysis with suitable internal reference. The yields are determined by ^{1}H NMR spectroscopy analysis using reference substance (isolated yields are given in parentheses). For details, see Experimental Section.
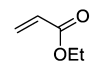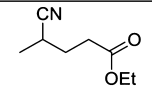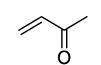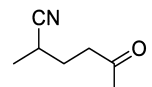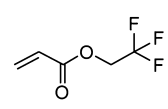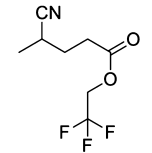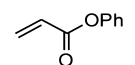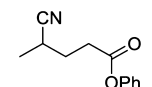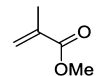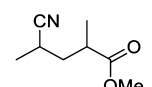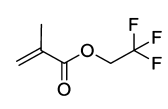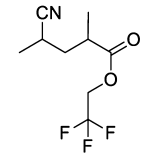
The overall barrier for this tautomerization via protonation/deprotonation of complex **6** is 32.6 kcal/mol. Since previous DFT studies revealed that water as proton shuttle can be essential for related transformations in transition metal complexes with pincer ligands, we furthermore computed an alternative mechanism with water molecules as proton shuttle.[48] A transition state with two water molecules (**TS3**) was found to lower the barrier for tautomerization to 21.0 kcal/mol. Interestingly, further NMR and DFT investigations indicate that water can reversibly add to complex **4**, yielding a re-aromatized hydroxy complex. We therefore conclude that small amounts of water, only catalytic with respect to the cataly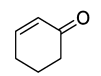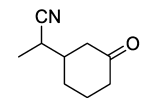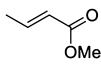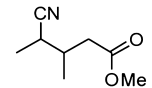st, are necessary to allow the tautomerization of **6**. On the other hand, larger amounts of water can deactivate the catalyst.[49] In agreement with the NMR investigations (see Figure 5), complex **7** is predicted to be less stable than complex **6** by 1.2 kcal/mol. To gain a deeper understanding of the metal template strategy, the nitrile⇌ketimine tautomerization of propionitrile itself was also calculated.

The calculations predict the nitrile form to be more stable by 22 kcal/mol (Scheme 7). Therefore, these results indicate that a first effect of the template strategy is the stabilization of the nucleophilic tautomer of the nitrile substrate. Having established a possible pathway for the formation of complex

7, we turned our attention to the C−C bond formation. We assumed that hydrogen bond interactions may stabilize the zwitterionic intermediate, which results from the nucleophilic attack of **7** at the Michael acceptor. Indeed, a transition state for the C−C bond formation with a hydrogen bond between the NH group of **7** and the carboxylic oxygen of ethyl acrylate could be localized (**TS4** in Figure 8). A proton transfer for which a relaxed potential energy surface scan over the OH bond length did not show a barrier led to the enol intermediate **13**, which is high in energy. We therefore searched for alternative pathways avoiding the intermediate enol formation. After attack of **7** via **TS5**, a zwitterionic intermediate **14** is formed. Its energy is lower than that of the enol intermediate **13**.

Rotation of the enolate group around the new carbon−carbon bond via the staggered transition state **TS6** leads to intermediate **15**. This intermediate can undergo a direct proton transfer from the NH group to the α-carbon of the enolate group via **TS7** to directly yield the keto intermediate **16**, thus avoiding the formation of the high energy enol intermediate **13**. A similar transition state as located for the binding of the propionitrile to **4** results in the product complex **17**. In this complex, the product is still bound to the manganese center via the nitrogen. Dissociation of the product finally regenerates the

Table 2. Michael Addition of Propionitrile to α,β-Unsaturated Carbonyl Compounds Catalyzed by Complex 4[a]

Entry	Acceptor	Time (h)	Conversion (%)	Yield (%)	Product
1		5	>99	93(71)	
2		2	>99	86(84)	
3		2	>99	93(71)	
4		26	58	52	
5		12	>99	92(92)	
6		5	>99	93(90)	
7		5	>99	33	
8		24	40	18	

[a]Reaction conditions: 1 mmol of substrates, ratio 1:1; 0.5 mol% complex **4**; ambient temperature; 0.5 mL of solvent (for entries 1−3, benzene; for entries 4−8, neat propionitrile). The conversion, with respect to the acceptor, is determined by ^{1}H NMR spectroscopic analysis. The yields were determined by ^{1}H NMR spectroscopic analysis using reference substance. Isolated yields are given in parentheses. For details, see Experimental Section.

active catalyst **4**. Notably, the pathway involving a zwitterionic intermediate not stabilized by hydrogen bonding is lower in energy than the one involving the enol intermediate. Regarding the overall transformation, the transition state for the water-assisted tautomerization is the one highest in energy with respect to the catalyst and the separated reactants. Remarkably, investigations on the temperature dependence of the catalytic reaction revealed that the reaction is faster at lower temperatures.[49] This is in agreement with the conclusion derived from the temperature-dependent NMR investigations and the DFT calculations that the binding of the propionitrile to the catalyst **4** is exothermic but endergonic.

On the basis of the NMR investigations and the DFT calculations, we propose the following mechanism to be operative (Scheme 8): Nitrile binding to complex **4** gives the ketimido compound **I**, and subsequently a water-assisted tautomerization takes place to give the enamido complex **II**.

The carbon−carbon bond formation yields a zwitterionic intermediate **III**. A proton transfer from the NH group leads directly to an intermediate in the keto form (**IV**). No enol intermediate is involved in the cycle. Product release regenerates the active de-aromatized catalyst **4**.

Essentially, the proposed catalytic cycle outlines a cascade of a stepwise reduction and oxidation of the CN bond. The formal bond order (b.o.) decreases in the course of the activation of the nitrile (nitrile (b.o. = 3) → ketimid (b.o. = 2) → enamid (b.o. = 1)). Upon addition of the reduced enamido moiety to the Michael acceptor, the CN bond order increases stepwise (ketimid (b.o. = 2) → nitrile (b.o. = 3).

■ SUMMARY AND CONCLUSIONS

The pincer complex *mer*-[Mn(PNP^{tBu})(CO)$_3$]Br (**2**), based on the abundant base-metal manganese, undergoes deprotonation
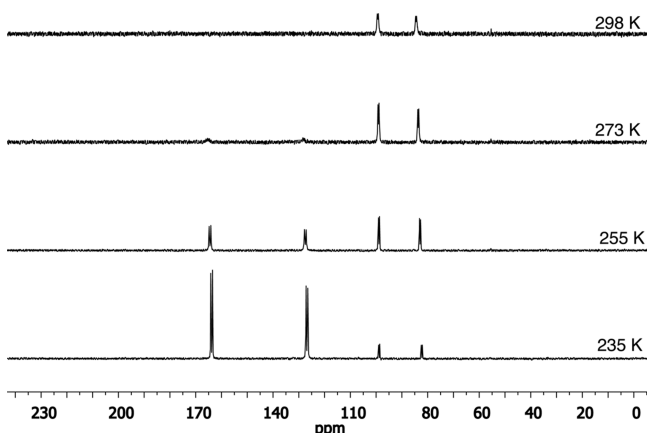
Figure 4. $^{31}P\{^1H\}$ NMR spectra at variable temperatures of complex **4** in n-pentane and 12 equiv of propionitrile.
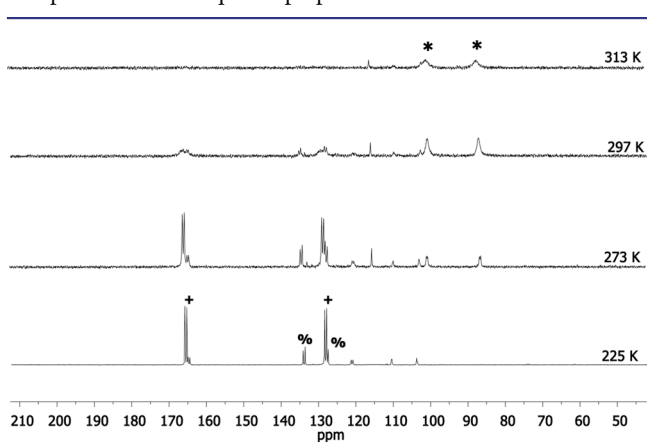

Figure 5. $^{31}P\{^1H\}$ NMR spectra at variable temperatures of complex **4** in neat propionitrile. Assignment: (*) = complex **4**; (+) = complex **6**; (%) = complex **7**.

upon treatment with a base to form the de-aromatized complex **4**, which reacts with nitrile triple bonds, forming *reversibly* C−C and Mn−N bonds. Based on this reactivity pattern, we have developed an unusually efficient Michael reaction catalyzed by complex **4** for the addition of non-activated nitriles to α,β-unsaturated carbonyl compounds. Remarkably, non-activated aliphatic nitriles can be used directly, for the first time, as Michael donor moieties under base-free and very mild conditions, which can react with a wide range of α,β-unsaturated carbonyl substrates in an atom-economic reaction.
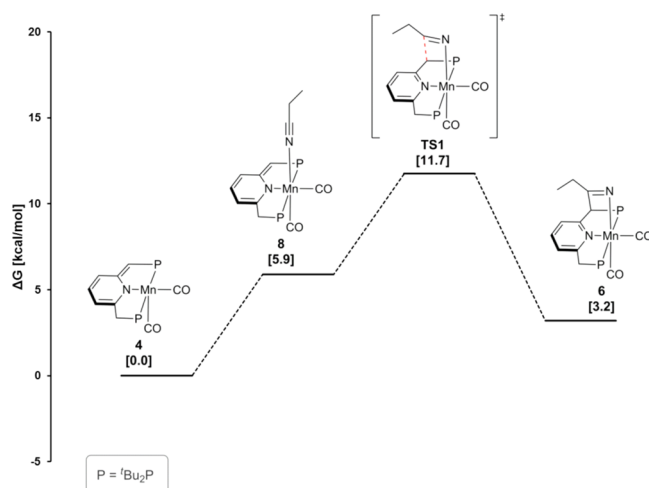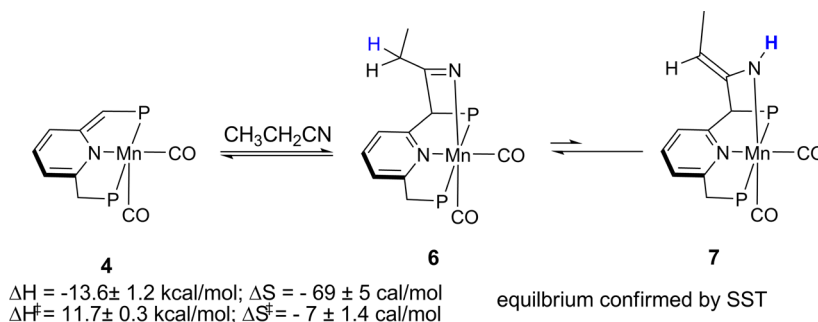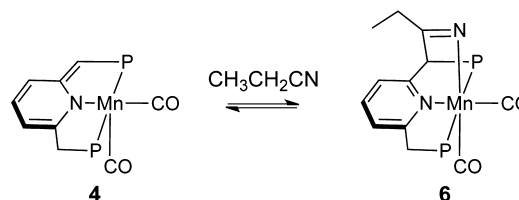

Figure 6. Pathway for the formation of **6**. Free energies (kcal/mol) with respect to the catalyst and the separated reactants calculated at the TPSS-D3BJ/def2-TZVP//BP86-D3/def2-SV(P) level of theory are given in brackets.

Scheme 6. Calculated Free Energies of the Propionitrile Binding to 4 at 298 and 235 K (P = $^tBu_2P$)

$\Delta G\ (298\ K) = 3.20\ kcal/mol$
$\Delta G\ (235\ K) = -0.04\ kcal/mol$

■ EXPERIMENTAL SECTION

All experiments were carried out in a M-BRAUN Unilab 1200/780 glovebox under inert atmosphere of purified nitrogen, or using standard Schlenk techniques. Tetrahydrofuran, toluene, benzene, dioxane and n-pentane were refluxed over sodium/benzophenone, distilled under argon atmosphere, and stored over 4 Å molecular sieves. Methylene chloride and acetonitrile were purchased from J. T. Baker as a Photrex reagent and as HPLC ultra gradient (respectively) and dried over 4 Å molecular sieves. Deuterated solvents were degassed with argon and kept in the glovebox over 4 Å molecular sieves. $[Mn(CO)_5Br]$ and KO^{t}Bu were purchased from Sigma-Aldrich and used as received. The PNP^{tBu} ligand was prepared according to the literature procedure.[50] Propionitrile, butyronitrile, benzylcyanide and valeronitrile were distilled and kept over 4 Å molecular sieves. All $[\alpha,\beta]$-unsaturated compounds were distilled or condensed before use

Scheme 5. Summary of the NMR Investigations of the Reaction of Complex 4 with Propionitrile (P = $^tBu_2P$)

4
$\Delta H = -13.6 \pm 1.2$ kcal/mol; $\Delta S = -69 \pm 5$ cal/mol
$\Delta H^{\ddagger} = 11.7 \pm 0.3$ kcal/mol; $\Delta S^{\ddagger} = -7 \pm 1.4$ cal/mol

6
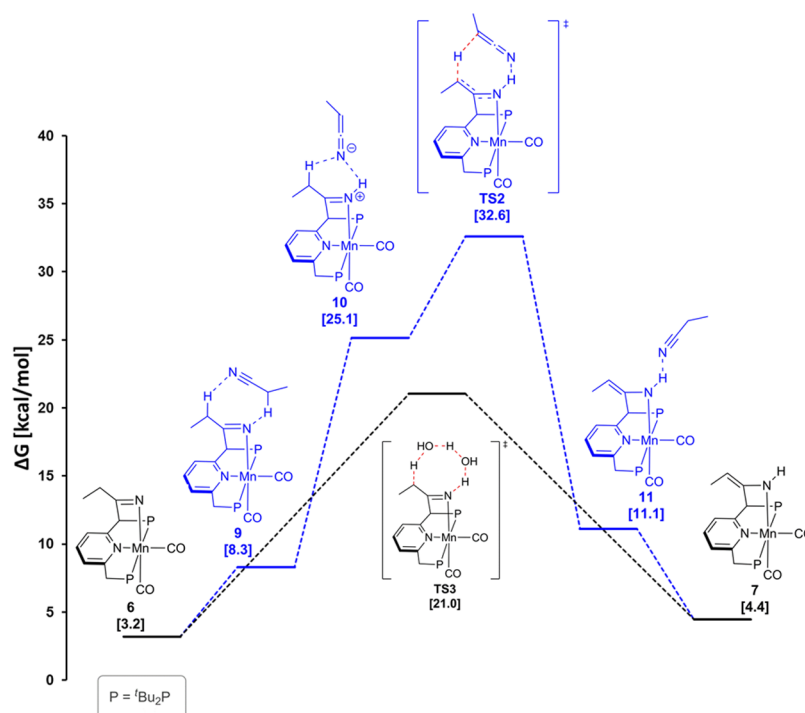
7
equilibrium confirmed by SST

Figure 7. Pathways for the tautomerization of **6**. Free energies with respect to **4** and the separated reactants calculated at the TPSS-D3BJ/def2-TZVP//BP86-D3/def2-SV(P) level of theory are given in brackets.

Scheme 7. Energy and Free Energy for the Nitrile↔Ketimine Tautomerization of Propionitrile Calculated at the TPSS-D3BJ/def2-TZVP//BP86-D3/def2-SV(P) Level (SMD for Benzene)

$$\Delta E + zpV \ (298 \ K) = 22.1 \ \text{kcal/mol}$$
$$\Delta G \ (298 \ K) \qquad = 22.0 \ \text{kcal/mol}$$
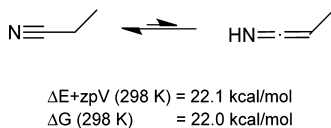
(purity was confirmed by NMR spectroscopy) and kept in −38 °C freezer inside the glovebox.

^{1}H, ^{13}C{^{1}H}, and ^{31}P{^{1}H} NMR spectra were recorded on Bruker AMX-300, AMX-400, and AMX-500 NMR spectrometers. ^{1}H, ^{13}C-{^{1}H}, and ^{13}C{^{1}H}-DEPTQ NMR chemical shifts are reported in ppm referenced to tetramethylsilane. ^{31}P{^{1}H} NMR chemical shifts are reported in ppm referenced to an external 85% solution of phosphoric acid in D$_2$O. IR spectra were recorded on a Nicolet FT-IR spectrophotometer. Mass spectra were recorded on a Micromass Platform LCZ 4000 instrument, using electrospray ionization mode. GC-MS was carried out on HP 6890/5973 (MS detector) instruments equipped with a 30 m column (Restek 5MS, 0.32 mm internal diameter) with a 5% phenylmethylsilicone coating (0.25 mm) and helium as carrier gas. Elemental analyses were performed on a ThermoFinnigan Italia S.p.A-FlashEA 1112 CHN elemental analyzer by the Department of Chemical Research Support, Weizmann Institute of Science.

Crystallographic details are as follows. For complex **4**: C$_{25}$H$_{42}$N$_1$O$_2$P$_2$Mn$_1$, black, 0.19 × 0.12 × 0.10 mm^3, orthorhombic, *Pbca* (No. 61), *a* = 11.723(2), *b* = 16.048(3), and *c* = 28.560(6) Å, from 20 degrees of data, *T* = 120(2) K, *V* = 5373.0(18) Å^3, *Z* = 8, FW = 505.48, *D*$_c$ = 1.250 mg·m^{-3}, μ = 0.631 mm^{-1}. Data collection and processing: Nonius Kappa CCD diffractometer, Mo Kα (λ = 0.71073 Å), graphite monochromator, 9254 reflections collected, −14 ≤ *h* ≤ 14, −19 ≤ *k* ≤ 19, −34 ≤ *l* ≤ 34, frame scan width = 1°, scan speed 1.0° per 120 s, typical peak mosaicity 0.66°, 4892 independent reflections (*R*-int = 0.0202). The data were processed with Denzo-Scalepack. Solution and refinement: Structure solved by direct

methods with SHELXS-97. Full-matrix least-squares refinement based on *F*^{2} with SHELXL-97; 296 parameters with 0 restraints, final *R*$_1$ = 0.0365 (based on *F*^{2}) for data with *I* > 2σ(*I*) and *R*$_1$ = 0.0492 on 4892 reflections, goodness-of-fit on *F*^{2} = 1.051, largest electron density peak = 0.650 Å^{-3}, deepest hole −0.301 Å^{-3}. For complex **5**: C$_{37}$H$_{57}$N$_2$O$_3$P$_2$Mn$_1$ (C$_{33}$H$_{49}$N$_2$O$_2$P$_2$Mn$_1$ + C$_4$H$_8$O$_1$), red, 0.20 × 0.13 × 0.12 mm^3, triclinic, *P*$\bar{1}$ (No. 2), *a* = 11.956(2), *b* = 12.902(3), and *c* = 13.400(3) Å, α = 116.17(3)°, β = 91.63(2)°, γ = 98.83(3)° from 20 degrees of data, *T* = 120(2) K, *V* = 1822.4(9) Å^3, *Z* = 2, FW = 694.73, *D*$_c$ = 1.266 mg·m^{-3}, μ = 0.487 mm^{-1}. Data collection and processing: Nonius Kappa CCD diffractometer, Mo Kα (λ = 0.71073 Å), graphite monochromator, 14 352 reflections collected, −14 ≤ *h* ≤ 15, −16 ≤ *k* ≤ 16, −16 ≤ *l* ≤ 16, frame scan width = 1°, scan speed 1.0° per 100 s, typical peak mosaicity 0.65°, 7693 independent reflections (*R*-int = 0.0324). The data were processed with Denzo-Scalepack. Solution and refinement: Structure solved by direct methods with SHELXS-97. Full matrix least-squares refinement based on *F*^{2} with SHELXL-97; 426 parameters with 1 restraint, final *R*$_1$ = 0.0430 (based on *F*^{2}) for data with *I* > 2σ(*I*) and *R*$_1$ = 0.0595 on 7693 reflections, goodness-of-fit on *F*^{2} = 1.054, largest electron density peak = 0.566 Å^{-3}, deepest hole −0.498 Å^{-3}.

Computational Methods. All geometries were optimized with the BP86 generalized-gradient approximation (GGA) functional and the def2-SV(P) basis set together with corresponding core potential for ruthenium.[51−54] The D3 dispersion correction was used for the geometry optimizations.[55] Thermodynamic properties were obtained at the same level of theory from a frequency calculation. All free energies are calculated under standard conditions unless otherwise noted. Minima and transition states were characterized by the absence and presence of one imaginary frequency, respectively. Single point calculations were obtained with the TPSS meta-GGA functional in combination with the D3 dispersion correction and Becke-Johnson dumping and the larger triple-ζ def2-TZVP basis set.[53,55−57] The TPSS functional was recently shown to yield results very close to explicitly correlated coupled cluster benchmark calculations for reaction energies and barriers involving transition metal complexes with pincer ligands.[58] In order to improve the computational efficient, the density fitting approximation with the W06 fitting basis sets, designed for use with the def2 basis sets, was used.[59,60] In order to take solvent effects into
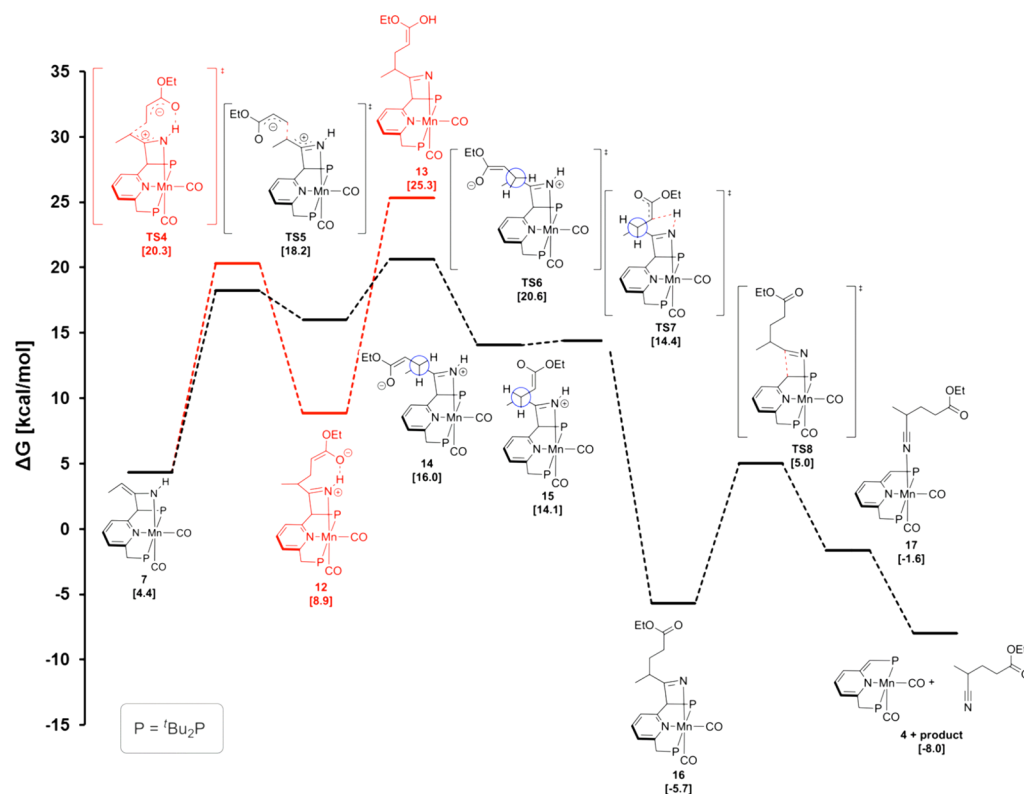
Figure 8. Pathway for product formation starting from the enamido complex **7**. For the intermediates **14** and **15** and the transition states **TS6** and **TS7**, the newly formed C−C bond is shown in a Newman projection. Free energies with respect to **4** and the separated reactants calculated at the TPSS-D3BJ/def2-TZVP//BP86-D3/def2-SV(P) level of theory are given in brackets.

Scheme 8. Simplified Catalytic Cycle for the Conjugate Addition of Unactivated Nitriles to Michael Acceptors Catalyzed by 4
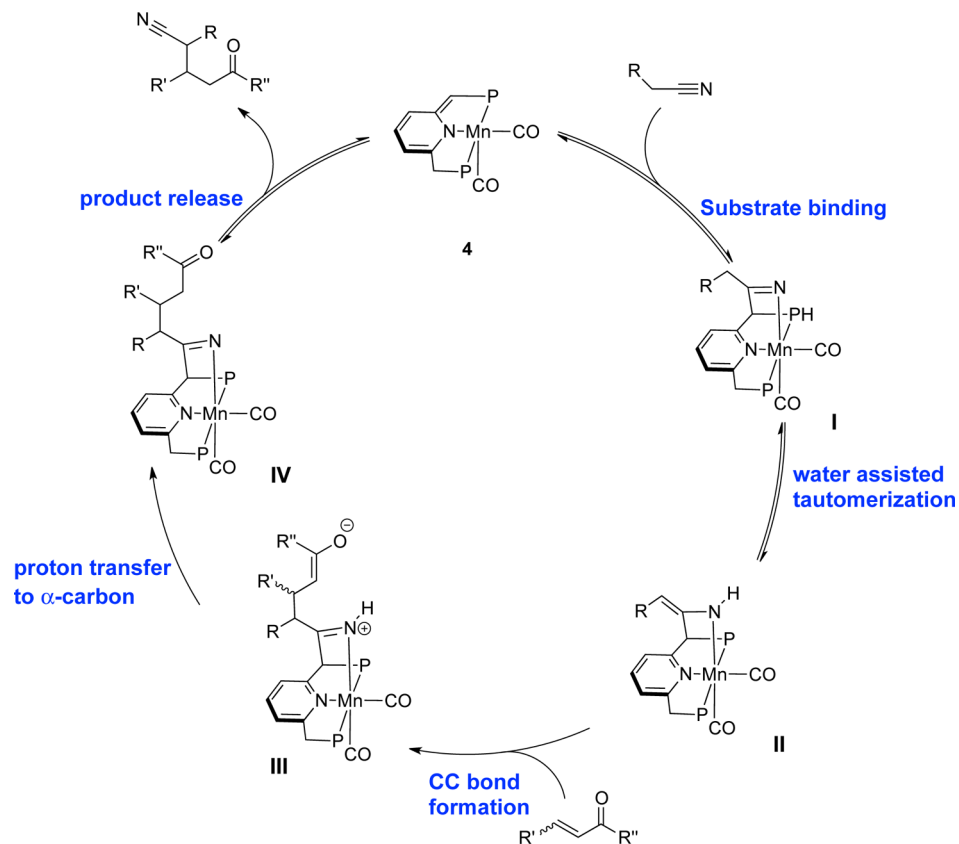
account, the SMD solvation model for benzene was used for both, the geometry optimizations and the single point calculations.[61] The "ultrafine" (i.e., a pruned (99,590)) grid was used for all calculations. All calculations were performed using Gaussian 09 Revision D.01.[62]

Syntheses. *mer-[Mn(PNP^{tBu})(CO)$_3$]Br (2).* 2,6-Bis(di-*tert*-butyl-phosphinomethyl)pyridine (PNP$^{t\text{-}Bu}$ ligand) (537 mg, 1.36 mmol) was dissolved in 9 mL of benzene and added to a stirred suspension of [Mn(CO)$_5$Br] (380 mg, 1.36 mmol) in 9 mL of benzene in a 20 mL vial. The mixture was stirred at room temperature for 30 h. The obtained suspension was distributed equally between three vials, which were subsequently layered with *n*-pentene and kept at −38 °C. The yellow precipitate was decanted, washed with *n*-pentane, and dried under reduced pressure (700 mg, 83% yield). ^{31}P{^{1}H} NMR (162.07 MHz, (CD$_3$)$_2$SO, 25 °C): δ 109.37 (s, 2P). ^{1}H NMR (400.36 MHz, (CD$_3$)$_2$SO, 25 °C): δ 1.35 (d, $^3J_{PH}$ = 12.7 Hz, 36H, (CH$_3$)$_3$CP), 4.07 (d, $^2J_{HP}$ = 7.0 Hz, 4H, PCH$_2$), 7.65 (d, $^3J_{HH}$ = 7.7 Hz, 2H, CH$_{pyri(3,5)}$), 7.94 (t, $^3J_{HH}$ = 7.7 Hz, 1H, CH$_{pyri(4)}$). ^{13}C{^{1}H} QDEPT NMR (100.67 MHz, (CD$_3$)$_2$SO, 25 °C): δ 29.74 (s, 12C, (CH3)$_3$CP), 36.76 (t, $^1J_{PC}$ = 6.7 Hz, 4C, (CH$_3$)$_3$CP), 38.34 (t, $^1J_{PC}$ = 8 0.0 Hz, 2C, CH$_2$P), 122.76 (s, 2C,CH$_{pyri(3,5)}$), 139.68 (s, 1C, CH$_{pyri(4)}$), 163.23 (s, 2C, CH$_{pyri(2,6)}$), 220.46 (t, $^2J_{PC}$ = 15.9 Hz, 2C, Mn-CO), 223.91 (t, $^2J_{PC}$ = 12.8 Hz, 1C, Mn-CO). IR (KBr, pellet, cm^{-1}): 1919, 1932 (overlapping) ($\nu_{3CO\ asymmetric}$ + $\nu'_{3CO\ asymmetric}$), 2021 ($\nu_{3CO\ symmetric}$) in 10:1 ratio. Elemental analysis (C$_{26}$H$_{43}$BrMnNO$_3$P$_2$) calculated (found): C, 50.83 (50.80); H, 7.05 (7.04); N, 2.28 (2.26)%.

mer-[Mn(PNP^{tBu}*)(CO)$_3$] (3). Method A, via de-aromatization of *mer*-[Mn(PNP^{tBu})(CO)$_3$]Br (2): *mer*-[Mn(PNP^{tBu})(CO)$_3$]Br (2) (50 mg, 0.08 mmol) was suspended in 4 mL of THF. KO^{t}Bu (33 mg, 0.30 mmol) was dissolved in 2 mL of THF and added dropwise to the suspension, which dissolved completely to give a brown homogeneous solution. The solution was allowed to stir for 0.5 h at ambient temperature. Subsequently all volatiles were evaporated in vacuo. The remaining brown residue was extracted with *n*-pentane (∼10 mL) and filtered through a Teflon syringe filter (0.2 μm porosity). Brown crystals and amorphous precipitate were formed upon storing the solution at −38 °C for 48 h. The solids were decanted and dried under reduced pressure to yield 38 mg of a 2:1 mixture of *mer*-[Mn(PNP^{tBu}*)(CO)$_3$] (3) and *cis*-[Mn(PNP^{tBu}*)(CO)$_2$] (4). Method B, via CO addition to *cis*-[Mn(PNP^{tBu}*)(CO)$_2$] (4): *cis*-[Mn(PNP^{tBu}*)(CO)$_2$] (4) (8 mg, 0.016 mmol) was dissolved in 0.5 mL of C$_6$D$_6$ and transferred to a J. Young NMR tube with Kontes valve. The tube was degassed and subsequently filled with 1 atm of CO gas, which resulted in a color change from dark blue to orange. Analysis by multinuclear NMR spectroscopy indicated the quantitative formation of *mer*-[Mn(PNP^{tBu}*) (CO)$_3$] (3). ^{31}P{^{1}H} NMR (162.07 MHz, C$_6$D$_6$, 25 °C): δ 100.84 (br, 1P), 108.34 (br, 1P). ^{1}H NMR (400.36 MHz, C$_6$D$_6$, 25 °C): δ 1.11 (d, $^3J_{PH}$ = 12.4 Hz, 18H, (CH$_3$)$_3$CP), 1.45 (d, $^3J_{PH}$ = 12.6 Hz, 18H, (CH$_3$)$_3$CP), 2.73 (d, $^2J_{HP}$ = 8.1 Hz, 2H, PCH$_2$), 3.78 (s, 1H, PCH), 5.54 (d, $^3J_{HH}$ = 6.4 Hz, 1H, CH$_{pyri(3)}$), 6.25 (d, $^3J_{HH}$ = 8.7 Hz,1H, CH$_{pyri(5)}$), 6.48 (t, $^3J_{HH}$ = 7.3 Hz, 1H, CH$_{pyri(4)}$).^{13}C{^{1}H} QDEPT NMR (100.67 MHz, C$_6$D$_6$, 25 °C): δ 30.49 (s, 12C, (CH$_3$)$_3$CP), 31.19 (s, 12C, (CH$_3$)$_3$CP), 37.29 (d, $^1J_{PC}$ = 14.1 Hz, 1C, CH$_2$P), 37.64 (d, $^1J_{PC}$ = 11.5 Hz, 2C, (CH$_3$)$_3$CP), 39.94 (d, $^1J_{PC}$ = 17.2 Hz, 2C, (CH$_3$)$_3$CP), 67.52 (d, $^1J_{PC}$ = 40.2 Hz, 1C, CHP), 102.11 (d, $^3J_{PC}$ = 7.6 Hz, 1C, CH$_{pyri(3)}$), 113.08 (d, $^3J_{PC}$ = 15.0 Hz, 1C, CH$_{pyri(5)}$), 131.96 (s, 1C, CH$_{pyri(4)}$),157.85 (s, 1C, C$_{pyri(6)}$), 171.75 (d, $^2J_{PC}$ = 17.2 Hz, 21.0 Hz, 1C, C$_{pyri(2)}$), 224.66 (br, 2C, Mn-CO), 226.27 (br, 1C, Mn-CO). IR (KBr, pellet, cm^{-1}): 1884, 1924, 2020 (($\nu_{3CO\ antisymmetric}$ + $\nu_{3CO\ antisymmetric}$) + $\nu_{3CO\ symmetric}$ in 10:10:1 ratio). Elemental analysis (C$_{26}$H$_{42}$MnNO$_3$P$_2$) calculated (found): C, 58.53 (59.27); H, 7.94 (8.25); N, 2.63 (2.60)%.

cis-[Mn(PNP^{tBu}*)(CO)$_2$] (4). *mer*-[Mn(PNP^{tBu})(CO)$_3$]Br (2) (150 mg, 0.24 mmol) was suspended in 7 mL of THF. KO^{t}Bu (27 mg, 0.24 mmol) was dissolved in 5 mL of THF and added dropwise to the suspension to give a brown solution. The solution was subsequently transferred to a Schlenk tube. The closed vessel was heated (oil-bath temperature of 90 °C) and purged 10 times in 5 min intervals with a stream of argon followed by carful degassing under reduced pressure. Eventually the solvent was removed completely under reduced pressure. The resulting dark blue powder was dissolved in 10 mL of

n-pentane and filtered through a Teflon syringe filter (0.2 μm). The solution was kept at −38 °C in a freezer for 48 h to form dark blue crystals. The crystals were decanted and dried under vacuum. (77 mg, 60% yield). ^{31}P{^{1}H} NMR (202.5 MHz, C$_6$D$_6$, 25 °C): δ 87.15 (d, $^2J_{PP}$ = 68.2 Hz, 1P, PCH=C), 101.30 (d, $^2J_{PP}$ = 68.1 Hz, 1P, PCH$_2$C). ^{1}H NMR (500.13 MHz, C$_6$D$_6$, 25 °C): 1.00 (d, $^3J_{PH}$ = 12.7 Hz, 18H, (CH$_3$)$_3$CP), 1.28 (d, $^3J_{PH}$ = 13.0 Hz, 18H, (CH$_3$)$_3$CP), 2.77 (d, $^2J_{HP}$ = 9.2 Hz, 2H, PCH$_2$), 3.82 (s, 1H, PCH), 5.45 (d, $^3J_{HH}$ = 5.9 Hz, 1H, CH$_{pyri(3)}$), 6.36 (m, 1H, CH$_{pyri(4)}$), 6.40 (m, 1H, CH$_{pyri(5)}$). ^{13}C{^{1}H} QDEPT NMR (125.76 MHz, C$_6$D$_6$, 25 °C): 29.34 (d, $^2J_{CP}$ = 3.9 Hz, 6C, (CH$_3$)$_3$CP), 29.92 (d, $^2J_{CP}$ = 3.8 Hz, 6C, (CH$_3$)$_3$CP), 34.88 (d, $^1J_{CP}$ = 13.4 Hz, 1C, PCH$_2$), 36.11 (d, $^1J_{CP}$ = 13.7 Hz, 2C, (CH$_3$)$_3$CP), 37.65 (d, $^1J_{CP}$ = 21.6 Hz, 2C, (CH$_3$)$_3$CP), 71.42 (d, $^1J_{CP}$ = 43.9 Hz, 1C, PCH=C), 99.50 (d, $^2J_{PC}$ = 10.1 Hz, 1C,CH$_{pyri(3)}$), 117.06 (d, $^3J_{PC}$ = 17.3 Hz, 1C,CH$_{pyri(5)}$), 132.06 (s, 1C, CH$_{pyri(4)}$), 160.93 (dd, $^{2,3}J_{PC}$ = 5.2 Hz, 8.4 Hz, 1C, C$_{pyri(6)}$), 174.22 (dd, $^{2,3}J_{PC}$ = 5.8 Hz, 21.0 Hz, 1C,C$_{pyri(2)}$), 239.25(t, $^2J_{CP}$ = 17.3 Hz, 2C,Mn-CO). IR (KBr, pellet, cm^{-1}): 1833, 1904 ($\nu_{2CO\ symmetric}$ + $\nu_{2CO\ antisymmetric}$, 1:1 ratio). Elemental analysis (C$_{25}$H$_{42}$MnNO$_2$P$_2$) calculated (found): C, 59.40 (59.72); H, 8.37 (8.46); N, 2.77 (2.70)%.

cis-[Mn(PNP^{tBu}-NHC=CHPh)(CO)$_2$] (5). *cis*-Mn(PNP^{tBu}*)-(CO)$_2$(4) (22 mg, 0.043 mmol) was dissolved in 1 mL of THF in a 20 mL vial. Subsequently, benzyl cyanide (10 mg, 0.085 mmol) was added resulting in a color change of the solution from dark blue to red. The solution was layered with 4 mL of *n*-pentane and kept at −38 °C in the freezer for 48 h. The formed large red crystals were decanted, washed with *n*-pentane, and dried under reduced pressure (23 mg, 85% yield). ^{31}P{^{1}H} NMR (162.07 MHz, C$_6$D$_6$, 25 °C): δ 126.64 (d, $^2J_{PP}$ = 98.6 Hz, 1P), 140.14 (d, $^2J_{PP}$ = 100.7 Hz, 1P). ^{1}H NMR (400.36 MHz, C$_6$D$_6$, 25 °C): δ 0.69 (d(br), $^3J_{PH}$ = 10.7 Hz, 9H, (CH$_3$)$_3$CP), 1.00 (d, $^3J_{PH}$ = 10.5 Hz, 9H, (CH$_3$)$_3$CP), 1.39 (d, $^3J_{PH}$ = 12.1 Hz, 9H, (CH$_3$)$_3$CP), 1.58 (d, $^3J_{PH}$ = 11.7 Hz, 9H, (CH$_3$)$_3$CP), 2.76 (dd, $^2J_{HH}$ = 16.1 Hz $^2J_{HP}$ = 10.2 Hz, 1H, (CH$_2$)P), 3.21 (dd, $^2J_{HH}$ = 16.0 Hz $^2J_{HP}$ = 3.7 Hz, 1H, (CH$_2$)P), 4.09 (d, $^2J_{HP}$ = 9.3 Hz, 1H, PCH), 4.39 (s, 1H, Mn−NH), 5.41 (s, 1H, Ph−CH=C), 6.35 (d, $^3J_{HH}$ = 7.6 Hz, 1H, CH$_{(pyridine(3))}$), 6.73 (d, $^3J_{HH}$ = 7.6 Hz, 1H, CH$_{(pyridine(5))}$), 6.82 (t, $^3J_{HH}$ = 7.6 Hz, 1H, CH$_{(pyridine(4))}$), 6.90 (t, $^3J_{HH}$ = 7.3 Hz, 1H, CH$_{(aryl-para)}$), 7.29 (t, $^3J_{HH}$ = 7.7 Hz, 2H, CH$_{(aryl-meta)}$), 7.49 (d, $^3J_{HH}$ = 7.7 Hz, 2H, CH$_{(aryl-ortho)}$). ^{13}C{^{1}H} NMR (100.67 MHz, C$_6$D$_6$, 25 °C): δ 30.02 (br, 3C, (CH$_3$)$_3$CP), 30.76, 30.98, 31.17 (3 peaks overlapping, 9C, (CH$_3$)$_3$CP), 36.84 (br, 2C, (CH$_3$)$_3$CP), 37.20 (d, $^1J_{PC}$ = 11.8 Hz, 1C, PCH$_2$), 37.81 (m, 2C, (CH$_3$)$_3$CP), 63.25 (d, $^1J_{PC}$ = 9.9 Hz, 1C, PCH), 91.19 (s, 1C, Ph-CH=C), 118.34 (d, $^2J_{PC}$ = 6.6 Hz, 1CCH$_{(pyridine(3))}$), 118.79 (d, $^2J_{PC}$ = 5.9 Hz, 1CCH$_{(pyridine(5))}$), 119.79 (s, 1C, CH$_{(aryl-para)}$), 123.30 (s, 2C, CH$_{(aryl-ortho)}$), 128.70 (s, 2C, CH$_{(aryl-meta)}$), 136.10 (d, $^2J_{PC}$ = 5.9 Hz, 1C CH$_{(pyridine(4))}$), 144.03 (s, 1C, C$_{ipso(aryl)}$), 154.31 (d, $^2J_{PC}$ = 9.2 Hz, 1C, C$_{ipso\ (pyridine)}$), 161.00 (d, $^2J_{PC}$ = 4.9 Hz, 1C, C$_{ipso(pyridine)}$), 165.18 (m, 1C, CH=C-NH), 232.83 (br, 1C, Mn-CO), 234.92 (br, 1C, Mn−CO). IR (KBr, pellet, cm^{-1}): 1832, 1905 ($\nu_{2CO\ symmetric}$ + $\nu_{2CO\ antisymmetric}$, 1:1 ratio). Elemental analysis (C$_{33}$H$_{49}$MnN$_2$O$_2$P$_2$) calculated (found): C, 63.66 (64.25); H, 7.93 (8.24); N, 4.50 (4.11)%.

Procedure for the Catalytic Reactions of Aliphatic Nitriles and Benzyl Cyanide with α,β-Unsaturated Esters and Ketones. *Procedure A (with Additional Solvent).* A stock solution containing 5 mg/mL (0.01 mmol/mL) of *cis*-[Mn(PNP^{tBu}*)(CO)$_2$] (4) in the particular reaction media (solvent: C$_6$H$_6$, THF, DCM, or *n*-pentane) was prepared. To 0.5 mL of the stock solution (0.005 mmol catalyst) 1 mmol of nitrile was added followed by the addition of 1 mmol of the specific α,β-unsaturated compound. The mixture stirred at room temperature (∼22 °C) for the indicated time and quenched by introduction of non-dried*n*-pentane. The yield was determined by integration of ^{1}H NMR signals with respect to the suitable standard, either toluene for the reaction in THF, dichloromethane, and *n*-pentane, or dioxane for C$_6$H$_6$ (the standard was added before quenching). The products were purified according to the indicated method, and isolated yields are reported; for details, see Supporting Information.

Procedure B (Neat Nitrile). A stock solution of propionitrile containing 5 mg/mL (0.01 mmol/mL) of *cis*-[Mn(PNP^{tBu}*)(CO)$_2$]

(**4**) was prepared. To 0.5 mL of stock solution (0.005 mmol catalyst) 1 mmol of the specific α,β-unsaturated compound was added. The mixture was stirred at room temperature ($\sim$22 °C) for the indicated time and quenched by introduction of non-dried *n*-pentane. The yield was determined by integration of ^{1}H NMR signals with respect to toluene as an external standard. The products were purified according to the indicated method, isolated yields are reported; for details, see Supporting Information.

ASSOCIATED CONTENT

Ⓢ Supporting Information

The Supporting Information is available free of charge on the ACS Publications website at DOI: 10.1021/jacs.5b13208.

> NMR spectra, experimental details, and characterization data (PDF)
> X-ray crystallographic data for **4** and **5** (CIF)

AUTHOR INFORMATION

Corresponding Author
*david.milstein@weizmann.ac.il

Author Contributions
§A.N., M.V., and U.G. contributed equally.

Notes
The authors declare no competing financial interest.

ACKNOWLEDGMENTS

REFERENCES

(1) Perlmutter, P.; Baldwin, J. E. *Conjugate Addition Reactions in Organic Synthesis*; Elsevier Science: Amsterdam, 2013.

(2) Christoffers, J. *Eur. J. Org. Chem.* **1998**, *1998*, 1259.

(3) Comelles, J.; Moreno-Mañas, M.; Vallribera, A. *Arkivoc* **2005**, 207.

(4) Fleming, F. F.; Yao, L.; Ravikumar, P. C.; Funk, L.; Shook, B. C. *J. Med. Chem.* **2010**, *53*, 7902.

(5) Takaya, H.; Ito, M.; Murahashi, S.-I. *J. Am. Chem. Soc.* **2009**, *131*, 10824.

(6) Fleming, F. F.; Vu, V. A.; Shook, B. C.; Rahman, M.; Steward, O. W. *J. Org. Chem.* **2007**, *72*, 1431.

(7) Murahashi, S.-I.; Naota, T.; Taki, H.; Mizuno, M.; Takaya, H.; Komiya, S.; Mizuho, Y.; Oyasato, N.; Hiraoka, M. *J. Am. Chem. Soc.* **1995**, *117*, 12436.

(8) Naota, T.; Tannna, A.; Murahashi, S.-I. *J. Am. Chem. Soc.* **2000**, *122*, 2960.

(9) Aydin, J.; Conrad, C. S.; Szabó, K. J. *Org. Lett.* **2008**, *10*, 5175.

(10) Naota, T.; Taki, H.; Mizuno, M.; Murahashi, S. *J. Am. Chem. Soc.* **1989**, *111*, 5954.

(11) Fleming, F. F.; Liu, W.; Ghosh, S.; Steward, O. W. *J. Org. Chem.* **2008**, *73*, 2803.

(12) Hoz, S.; Albeck, M.; Rappoport, Z. *Synthesis* **1975**, *1975*, 162.

(13) Hasegawa, Y.; Watanabe, M.; Gridnev, I. D.; Ikariya, T. *J. Am. Chem. Soc.* **2008**, *130*, 2158.

(14) Lopez, R.; Palomo, C. *Angew. Chem., Int. Ed.* **2015**, *54*, 13170.

(15) Vogt, M.; Nerush, A.; Iron, M. A.; Leitus, G.; Diskin-Posner, Y.; Shimon, L. J. W.; Ben-David, Y.; Milstein, D. *J. Am. Chem. Soc.* **2013**, *135*, 17004.

(16) Filonenko, G. A.; Cosimi, E.; Lefort, L.; Conley, M. P.; Copéret, C.; Lutz, M.; Hensen, E. J. M.; Pidko, E. A. *ACS Catal.* **2014**, *4*, 2667.

(17) Perdriau, S.; Zijlstra, D. S.; Heeres, H. J.; de Vries, J. G.; Otten, E. *Angew. Chem., Int. Ed.* **2015**, *54*, 4236.

(18) Kariyone, K. *Chem. Pharm. Bull.* **1960**, *8*, 1110.

(19) Albrecht, M.; Lindner, M. M. *Dalton Trans.* **2011**, *40*, 8733.

(20) Albrecht, M.; van Koten, G. *Angew. Chem., Int. Ed.* **2001**, *40*, 3750.

(21) Gunanathan, C.; Milstein, D. *Acc. Chem. Res.* **2011**, *44*, 588.

(22) Gunanathan, C.; Milstein, D. *Top. Organomet. Chem.* **2011**, *37*, 55.

(23) van der Vlugt, J. I. *Eur. J. Inorg. Chem.* **2012**, *2012*, 363.

(24) van der Vlugt, J. I.; Reek, J. N. H. *Angew. Chem., Int. Ed.* **2009**, *48*, 8832.

(25) *The Chemistry of Pincer Compounds*; Morales-Morales, D., Jensen, M. C., Eds.; Elsevier: Amsterdam, 2007; pp 1−467.

(26) Milstein, D. *Philos. Trans. R. Soc., A* **2015**, *373*, 20140189.

(27) Feller, M.; Diskin-Posner, Y.; Shimon, L. J. W.; Ben-Ari, E.; Milstein, D. *Organometallics* **2012**, *31*, 4083.

(28) Khaskin, E.; Iron, M. A.; Shimon, L. J. W.; Zhang, J.; Milstein, D. *J. Am. Chem. Soc.* **2010**, *132*, 8542.

(29) Kohl, S. W.; Weiner, L.; Schwartsburd, L.; Konstantinovski, L.; Shimon, L. J. W.; Ben-David, Y.; Iron, M. A.; Milstein, D. *Science* **2009**, *324*, 74.

(30) Schwartsburd, L.; Iron, M. A.; Konstantinovski, L.; Ben-Ari, E.; Milstein, D. *Organometallics* **2011**, *30*, 2721.

(31) Schwartsburd, L.; Iron, M. A.; Konstantinovski, L.; Diskin-Posner, Y.; Leitus, G.; Shimon, L. J. W.; Milstein, D. *Organometallics* **2010**, *29*, 3817.

(32) Ben-Ari, E.; Leitus, G.; Shimon, L. J. W.; Milstein, D. *J. Am. Chem. Soc.* **2006**, *128*, 15390.

(33) Prechtl, M. H. G.; Hölscher, M.; Ben-David, Y.; Theyssen, N.; Loschen, R.; Milstein, D.; Leitner, W. *Angew. Chem., Int. Ed.* **2007**, *46*, 2269.

(34) Kloek, S. M.; Heinekey, D. M.; Goldberg, K. I. *Angew. Chem., Int. Ed.* **2007**, *46*, 4736.

(35) Hanson, S. K.; Heinekey, D. M.; Goldberg, K. I. *Organometallics* **2008**, *27*, 1454.

(36) de Boer, S. Y.; Gloaguen, Y.; Lutz, M.; van der Vlugt, J. I. *Inorg. Chim. Acta* **2012**, *380*, 336.

(37) van der Vlugt, J. I.; Pidko, E. A.; Bauer, R. C.; Gloaguen, Y.; Rong, M. K.; Lutz, M. *Chem. - Eur. J.* **2011**, *17*, 3850.

(38) van der Vlugt, J. I.; Lutz, M.; Pidko, E. A.; Vogt, D.; Spek, A. L. *Dalton Trans.* **2009**, 1016.

(39) Vogt, M.; Gargir, M.; Iron, M. A.; Diskin-Posner, Y.; Ben-David, Y.; Milstein, D. *Chem. - Eur. J.* **2012**, *18*, 9194.

(40) Vogt, M.; Nerush, A.; Diskin-Posner, Y.; Ben-David, Y.; Milstein, D. *Chem. Sci.* **2014**, *5*, 2043.

(41) Montag, M.; Zhang, J.; Milstein, D. *J. Am. Chem. Soc.* **2012**, *134*, 10325.

(42) Huff, C. A.; Kampf, J. W.; Sanford, M. S. *Chem. Commun.* **2013**, *49*, 7147.

(43) Huff, C. A.; Kampf, J. W.; Sanford, M. S. *Organometallics* **2012**, *31*, 4643.

(44) Filonenko, G. A.; Conley, M. P.; Copéret, C.; Lutz, M.; Hensen, E. J. M.; Pidko, E. A. *ACS Catal.* **2013**, *3*, 2522.

(45) Radosevich, A. T.; Melnick, J. G.; Stoian, S. A.; Bacciu, D.; Chen, C.-H.; Foxman, B. M.; Ozerov, O. V.; Nocera, D. G. *Inorg. Chem.* **2009**, *48*, 9214.

(46) Umehara, K.; Kuwata, S.; Ikariya, T. *Inorg. Chim. Acta* **2014**, *413*, 136.

(47) Russell, S. K.; Bowman, A. C.; Lobkovsky, E.; Wieghardt, K.; Chirik, P. J. *Eur. J. Inorg. Chem.* **2012**, *3*, 535.

(48) (a) Iron, M. A.; Ben-Ari, E.; Cohen, R.; Milstein, D. *Dalton Trans.* **2009**, 9433. (b) Qu, S.; Dang, Y.; Song, C.; Wen, M.; Huang, K.; Wang, Z. *J. Am. Chem. Soc.* **2014**, *136*, 4974−4991.

(49) For details on this investigation, see the Supporting Information.

(50) Hermann, D.; Gandelman, M.; Rozenberg, H.; Shimon, L. J. W.; Milstein, D. *Organometallics* **2002**, *21*, 812.

(51) Becke, A. D. *Phys. Rev. A: At., Mol., Opt. Phys.* **1988**, *38*, 3098.

(52) Perdew, J. P. *Phys. Rev. B: Condens. Matter Mater. Phys.* **1986**, *33*, 8822.

(53) Weigend, F.; Ahlrichs, R. *Phys. Chem. Chem. Phys.* **2005**, *7*, 3297.

(54) Dolg, M. In *Modern Methods and Algorithms of Quantum Chemistry*; Grotendorst, J., Ed.; John von Neumann Institute for Computing: Julich, 2000; Vol. 3, pp 507.

(55) Grimme, S.; Antony, J.; Ehrlich, S.; Krieg, H. *J. Chem. Phys.* **2010**, *132*, 154104.

(56) Tao, J. M.; Perdew, J. P.; Staroverov, V. N.; Scuseria, G. E. *Phys. Rev. Lett.* **2003**, *91*, 146401.

(57) Johnson, E. R.; Becke, A. D. *J. Chem. Phys.* **2006**, *124*, 174104.

(58) Kesharwani, M. K.; Martin, J. M. L. *Theor. Chem. Acc.* **2014**, *133*, 1452.

(59) (a) Dunlap, B. I. *J. Chem. Phys.* **1983**, *78*, 3140. (b) Dunlap, B. I. *J. Mol. Struct.: THEOCHEM* **2000**, *529*, 37.

(60) Weigend, F. *Phys. Chem. Chem. Phys.* **2006**, *8*, 1057.

(61) Marenich, A. V.; Cramer, C. J.; Truhlar, D. G. *J. Phys. Chem. B* **2009**, *113*, 6378.

(62) Frisch, M. J.; Trucks, G. W.; Schlegel, H. B.; Scuseria, G. E.; Robb, M. A.; Cheeseman, J. R.; Scalmani, G.; Barone, V.; Mennucci, B.; Petersson, G. A.; Nakatsuji, H.; Caricato, M.; Li, X.; Hratchian, H. P.; Izmaylov, A. F.; Bloino, J.; Zheng, G.; Sonnenberg, J. L.; Hada, M.; Ehara, M.; Toyota, K.; Fukuda, R.; Hasegawa, J.; Ishida, M.; Nakajima, T.; Honda, Y.; Kitao, O.; Nakai, H.; Vreven, T.; Montgomery, J. A., Jr.; Peralta, J. E.; Ogliaro, F.; Bearpark, M.; Heyd, J. J.; Brothers, E.; Kudin, K. N.; Staroverov, V. N.; Keith, T.; Kobayashi, R.; Normand, J.; Raghavachari, K.; Rendell, A.; Burant, J. C.; Iyengar, S. S.; Tomasi, J.; Cossi, M.; Rega, N.; Millam, J. M.; Klene, M.; Knox, J. E.; Cross, J. B.; Bakken, V.; Adamo, C.; Jaramillo, J.; Gomperts, R.; Stratmann, R. E.; Yazyev, O.; Austin, A. J.; Cammi, R.; Pomelli, C.; Ochterski, J. W.; Martin, R. L.; Morokuma, K.; Zakrzewski, V. G.; Voth, G. A.; Salvador, P.; Dannenberg, J. J.; Dapprich, S.; Daniels, A. D.; Farkas, O.; Foresman, J. B.; Ortiz, J. V.; Cioslowski, J.; Fox, D. J. *Gaussian 09*, Revision D.01; Gaussian, Inc.: Wallingford, CT, 2013.